Pea2 Protein of Yeast Is Localized to Sites of Polarized Growth and Is Required for Efficient Mating and Bipolar Budding

Nicole Valtz and Ira Herskowitz

Department of Biochemistry and Biophysics, University of California, San Francisco, California 94143-0448

Abstract. *Saccharomyces cerevisiae* exhibits polarized growth during two phases of its life cycle, budding and mating. The site for polarization during vegetative growth is determined genetically: **a** and α haploid cells exhibit an axial budding pattern, and **a**/α diploid cells exhibit a bipolar pattern. During mating, each cell polarizes towards its partner to ensure efficient mating. *SPA2* is required for the bipolar budding pattern (Snyder, M. 1989. *J. Cell Biol.* 108:1419–1429; Zahner, J.A., H.A. Harkins, and J.R. Pringle. 1996. *Mol. Cell. Biol.* 16:1857–1870) and polarization during mating (Snyder, M., S. Gehrung, and B.D. Page. 1991. *J. Cell Biol.* 114: 515–532). We previously identified mutants defective in *PEA2* and *SPA2* which alter cell polarization in the presence of mating pheromone in a similar manner (Chenevert, J., N. Valtz, and I. Herskowitz. 1994. *Genetics.* 136:1287–1297). Here we report the further characterization of these mutants. We have found that *PEA2* is also required for the bipolar budding pattern and that it encodes a novel protein with a predicted coiled-coil domain. Pea2p is expressed in all cell types and is localized to sites of polarized growth in budding and mating cells in a pattern similar to Spa2p. Pea2p and Spa2p exhibit interdependent localization: Spa2p is produced in *pea2* mutants but fails to localize properly; Pea2p is not stably produced in *spa2* mutants. These results suggest that Pea2p and Spa2p function together as a complex to generate the bipolar budding pattern and to guarantee proper polarization during mating.

Cell polarity is an essential feature of many eukaryotic cell types. Neurons and epithelial cells are two examples of cells whose polarity is essential for their function. The ability to polarize is also critical for the budding yeast *Saccharomyces cerevisiae* to grow and to mate (for reviews see Drubin, 1991; Madden and Snyder, 1992; Chenevert, 1994). During vegetative growth, localization of all new material at a defined site on the cell surface leads to formation of the growing bud. During mating, the ability to recognize the position of the mating partner and polarize towards it results in the local deposition of mating-specific proteins and facilitates efficient cell and nuclear fusion (for a review see Cross et al., 1988).

Polarized growth in yeast depends on actin: disruption of the actin cytoskeleton by either depolymerizing drugs or by mutations leads to unlocalized growth (for a review see Welch et al., 1994). Two kinds of filamentous actin structures are found in yeast: patches, which cluster at sites of growth, and cables, which are found throughout the cell body directed towards the growth site (Adams and Pringle, 1984; Kilmartin and Adams, 1984). It is believed that secretory vesicles are targeted to growth sites by the actin cytoskeleton (Johnston et al., 1991).

During vegetative growth, the position of the bud (and thus the direction of polarized growth) is determined genetically: **a** and α haploid cells bud adjacent to the position of the previous bud (Chant and Pringle, 1995), in the axial budding pattern, and **a**/α diploid cells bud from either pole, in the bipolar budding pattern (Freifelder, 1960; Hicks et al., 1977; Sloat et al., 1981). A genetic hierarchy has been proposed to organize the actin cytoskeleton (Chant and Herskowitz, 1991). The bud site selection genes (including *RSR1/BUD1*, *BUD2-10*, *AXL1*, the neck filament genes, and many others) are required to position a bud at the specified site on the cell surface. The polarity establishment genes (such as *CDC42*, *CDC24*, and *BEM1*) are required to organize actin towards that site. Finally, the genes encoding actin and various actin-binding proteins are required to build the actin cytoskeleton. These gene products are proposed to cooperate to polarize growth towards the presumptive bud site: the *BUD* gene products organize the polarity establishment proteins towards the chosen site, and the polarity establishment proteins in turn organize the actin cytoskeleton.

In addition to growing vegetatively, yeast cells can mate to form a diploid when two haploid cells of opposite mat-

Please address all correspondence to I. Herskowitz, Department of Biochemistry and Biophysics, University of California, San Francisco, CA 94143-0448. Tel.: (415) 476-4977. Fax: (415) 502-5145.

© The Rockefeller University Press, 0021-9525/96/11/725/15 $2.00

ing type (**a** and α) come in contact (reviewed in Cross et al., 1988; Chenevert, 1994). During mating, cells ignore the polarity information at the presumptive bud site and polarize instead towards their mating partner (Madden and Snyder, 1992; Valtz et al., 1995): the actin and microtubule cytoskeletons as well as secretion and new cell surface growth are oriented towards the partner (Byers, 1981; Ford and Pringle, 1986; Hasek et al., 1987; Tkacz and MacKay, 1979). In this instance, the site for polarization is determined by an external signal, a gradient of pheromone secreted by the mating partner (Jackson and Hartwell 1990*a*,*b*; Segall, 1993; Dorer et al., 1995; Valtz et al., 1995). In the absence of a mating partner, mating pheromones induce polarization towards the presumptive bud site (Madden and Snyder, 1992; Valtz et al., 1995). The polarity establishment proteins, actin, and actin-binding proteins are also required during mating to generate an organized actin cytoskeleton (for review see Chenevert, 1994). Thus, the machinery for polarizing the actin cytoskeleton is common during budding and mating, but the sites for polarization are chosen by different mechanisms.

To identify genes involved in polarization during mating, we previously screened for mutants which mate poorly but which exhibit normal pheromone production and response (Chenevert et al., 1994). These mutants were characterized for their ability to polarize during mating by exposing **a** cells to mating pheromone from α cells. After several hours in pheromone, wild-type **a** cells form pear-shaped cells known as shmoos; after several more hours, wild-type cells extend a second shmoo tip. Several classes of mutants obtained in this screen were distinguished by their shmoo morphology. One class formed essentially wild-type shmoos after short exposure to pheromone, but over time the shmoo tip continued to grow, generating a peanut-shaped shmoo. The four mutants with this peanut morphology fell into two complementation groups; one of these complementation groups appeared novel and was named *PEA2*; the other was identified as the known gene *SPA2*.

SPA2 plays important roles in morphogenesis, but its exact functions remain obscure. *spa2* deletion mutants mate poorly (Gehrung and Snyder, 1990; Chenevert et al., 1994; Dorer et al., 1995) and form large unpolarized cells in the presence of pheromone (Gehrung and Snyder, 1990). *spa2* mutants also exhibit a bipolar budding pattern defect (Snyder, 1989; Zahner et al., 1996). Finally, *spa2* mutants display a cytokinesis defect, most evident in diploid cells (Snyder et al., 1991). *SPA2* encodes a 180-kD, nonessential protein with predicted coiled-coil domains that localizes to sites of polarized growth during budding and mating, where it might function in morphogenesis (Snyder, 1989; Gehrung and Snyder, 1990; Snyder et al., 1991).

Here we report the characterization of the *PEA2* gene and protein. We analyze the budding and mating phenotypes of *pea2Δ* strains and the expression and subcellular localization of Pea2p using an anti-Pea2p antibody. The behavior of Spa2p is also examined using an anti-Spa2p antibody. Our results suggest that Pea2p and Spa2p may function as a complex during two phases of polarized growth: establishment of the bipolar budding pattern and polarization during mating.

Materials and Methods

Materials

Spa2p antibodies were a generous gift from Mike Snyder (Yale University, New Haven, CT). α-Factor, Calcofluor, polylysine, and fluorescent secondary antibodies were from Sigma Chemical Co. (St. Louis, MO). Horseradish peroxidase–coupled antibodies and Affigel were from Bio-Rad Labs (Hercules, CA). Cyanogen bromide–activated Sepharose was from Pharmacia (Uppsala, Sweden).

Yeast Strains and Growth Conditions

Yeast strains and plasmids are described in Table I. Standard yeast growth conditions and genetic manipulations were used as described (Rose et al., 1990). Cells were grown at 30°C in rich YEPD medium unless otherwise noted.

Quantitative Mating and Shmoo Formation

Quantitative mating was essentially as described (Chenevert et al., 1994). In short, equal numbers of **a** and α cells (3×10^6) were mixed, filtered onto 0.45-μm filters, and incubated on permissive YEPD plates for 4 h at 30°C, allowing all cells to grow. Cells were resuspended in 5 ml minimal medium (SD) by vortexing followed by sonication and plated on permissive YEPD plates to determine total colony-forming units and on selective SD plates to determine the total number of diploids. Each experiment was carried out in triplicate at least twice.

Shmoo morphology was determined by the addition of 10^{-6}M α-factor to 3 ml log phase cultures. Aliquots were removed at 0, 2, and 6 h. Cells were sonicated, fixed to a final concentration of 5% formaldehyde, and viewed by differential interference contrast microscopy.

Budding Pattern Assays

Calcofluor staining of bud scars was performed as described (Pringle et al., 1989). **a** or α cells with a total of three or more bud scars were scored as axial if all bud scars were adjacent; other patterns were scored as nonaxial. **a**/α cells with a total of three or more bud scars at the two poles were scored as bipolar; all other patterns were scored as nonbipolar. For each sample, 400 cells were counted for at least two independent experiments.

Cloning and Sequencing of SPA2

We previously reported the identification of the mutants J9 and D6 as defective in *SPA2* (Chenevert et al., 1994) but did not describe the cloning which led to this conclusion. In brief, a centromere-based library (Rose et al., 1987) was transformed into the mutant J9 (NVY8), and transformants were screened for mating to an enfeebled mating partner carrying the mutation *far1-c* (JC31-7D). Of approximately 11,000 transformants screened, one plasmid (pNV8) rescued the mating and peanut shmoo morphology defects of both mutants D6 and J9 in a plasmid-dependent manner. To locate the complementing region within the 10-kilobase (kb) insert of pNV8, mini-Tn*10*-LUK transposons were introduced (Huisman et al., 1987). Insertions into the complementing open reading frame (ORF)[1] disrupted complementing activity. This new library of plasmids was transformed into the mutant J9, and transformants were again screened for the ability to mate with an enfeebled mating partner. Six plasmids which no longer complemented the J9 mating defect contained transposon insertions within a 2.8-kb SphI fragment. Sequencing the end of this fragment revealed *SPA2*. Deletion of the *SPA2* gene in the parent background generated a phenotype like that of the original mutant strains, further indicating that these mutants carry mutations in *SPA2*.

To determine whether the cloned DNA fragment corresponded to the mutated locus in the *pea1-1* mutant, an integrating vector (pNV10) was used to introduce a *URA3*-marked copy of the wild-type fragment into the *pea1-1* mutant; this strain was then crossed to the original *pea1-1* mutant. For 27 tetrads, the *pea1* mutant phenotype was found in the two Ura$^-$ segregants, indicating that the fragment carried the *PEA1* open reading frame (ORF).

1. *Abbreviation used in this paper*: ORF, open reading frame.

Table 1. Yeast Strains and Plasmids Used in This Study

Strain	Relevant genotype	Source
JC2-1B	*MATa HMLα HMRa bar1-1 met1-1 ade2-101 ura3-52*	Chenevert et al. (1994)
	The following strains are all isogenic to JC2-1B	
NVY6	*MATa pea2-1 bar1-1*	Chenevert et al. (1994)
NVY7	*MATa spa2-1 bar1-1*	Chenevert et al. (1994)
NVY8	*MATa spa2-1 bar1-1*	Chenevert et al. (1994)
NVY139	*MATa spa2::URA3 bar1-1*	This study
NVY201	*MATa pea2::URA3 bar1-1*	This study
NVY243	*MATa pea2::URA3 spa2::TRP1 trp1-Δ99 leu2-Δ1 bar1-1*	This study
NVY192	*MATα trp1-Δ99 leu2-Δ1*	This study
NVY193	*MATa trp1-Δ99 leu2-Δ1*	This study
NVY199	*MATα pea2::URA3 trp1-Δ99 leu2-Δ1*	This study
NVY200	*MATa pea2::URA3 trp1-Δ99 leu2-Δ1*	This study
NVY204	*MATα spa2::TRP1 trp1-Δ99 leu2-Δ1*	This study
NVY207	*MATa spa2::TRP1 trp1-Δ99 leu2-Δ1*	This study
NVY222	*MATa pea2-2 trp1-Δ99 leu2-Δ1*	This study
NVY226	*MATa pea2-1 trp1-Δ99 leu2-Δ1*	This study
NVY230	*MATa spa2-1 trp1-Δ99 leu2-Δ1*	This study
NVY233	*MATa spa2-2 trp1-Δ99 leu2-Δ1*	This study
NVY238	*MATα bni1::URA3 trp1-Δ99 leu2-Δ1*	This study
NVY239	*MATa bni1::URA3 trp1-Δ99 leu2-Δ1*	This study
NVY244	*MATa pea2::URA3 spa2::TRP1 trp1-Δ99*	This study
JPY142	*MATa/MATα trp1-Δ99/trp1-Δ99 leu2-Δ1/leu2-Δ1*	This study
NVY208	*MATa/MATα spa2::TRP1/spa2::TRP1 trp1-Δ99/trp1-Δ99 leu2-Δ1 leu2-Δ1*	This study
NVY210	*MATa/MATα pea2::URA3/pea2::URA3 trp1-Δ99/trp1-Δ99 leu2-Δ1/leu2-Δ1*	This study
NVY242	*MATa/MATα bni1::URA3/bni1::URA3 trp1-Δ99/trp1-Δ99 leu2-Δ1/leu2-Δ1*	This study
	Other strains	
IH1793	*MATα lys1*	IH collection
JC31-7D	*MATα far1-c lys1*	Chenevert et al. (1994)

Plasmid name	Description	Source
pNV8	Original J9 (*SPA2*) complementing clone	This study
pNV10	AatII fragment of pNV8 in YIp5	This study
pNV21	Original II4 (*PEA2*) complementing clone	This study
pNV22	SauIIIA fragment of pNV21 in pRS316	This study
pNV23	BamHI–XbaI fragment of pNV22 in pBLUESCRIPT	This study
pNV34	HindIII fragment of pNV22 in YCP50 with XhoI site digested and religated to generate a frameshift mutation	This study
pNV35	ApaI–HindIII fragment of pNV22 in pBLUESCRIPT	This study
pNV36	pNV35 with a replacement of the *PEA2* ORF with a SalI site introduced by PCR	This study
pNV44	*pea2::URA3* created by introducing the HindIII fragment of YIp31 into the SalI site of pNV36	This study
YIp31	*URA3* in pBR322	IH collection
p210	*spa2::URA3*	Mike Snyder
p211	*spa2::TRP1*	Mike Snyder
p321	*bni1::URA3*	Charlie Boone

Cloning and Sequencing of PEA2

PEA2 was cloned by complementation of its mating defect to a *far1-c* partner. A plasmid (pNV21) which rescued the mating and shmoo morphology defects of *pea2-1* (NVY6) was isolated from a centromeric library (Rose et al., 1987) and also rescued both phenotypes of a *pea2-2* mutant. The complementing plasmid, pNV21, contained an insert of ~13 kb. To further define the region carrying the *PEA2* gene, a library of partially digested SauIIIA fragments from pNV21 was constructed and transformed into the original *pea2-1* mutant. Two complementing plasmids (pNV22a and pNV22b) both carrying a 2.3-kb insert were recovered (Fig. 1 *C*); these plasmids contained the same DNA fragment in opposite orientations. Sequencing the end of a subclone of pNV22a (pNV23) revealed a 200-base pair fragment identical to a sequence in the Saccharomyces Genome Database.

To determine whether the cloned DNA fragment corresponded to the mutated locus in the *pea2-1* and *pea2-2* mutants, an integrating vector (pNV44) was used to introduce a *URA3*-marked copy of the wild-type fragment into both *pea2* mutants; these strains were then crossed to the original *pea2* mutants. For 18 tetrads, the *pea2* mutant phenotype was found in the two Ura$^-$ segregants, indicating that the fragment carried the *PEA2* ORF.

Two possible ORFs were found in the minimal complementing fragment, one 1.3 kb and the other 0.6 kb (Fig. 1 *B*). Because the smaller potential ORF was contained almost entirely within the larger ORF, but with the opposite orientation, it was important to determine which ORF encoded *PEA2*. To eliminate the smaller ORF, a mutation was introduced which interrupted the larger ORF at position 1779 but left the smaller ORF intact (pNV34). This plasmid failed to complement the mating and shmoo morphology defects of *pea2-1* and *pea2-2*, indicating that the larger ORF encodes *PEA2*. These sequence data are available from EMBL/GenBank/DDBJ under the accession number YO7594; *PEA2* is entered in the Saccharomyces Genome Database as YER149c.

Deletion of PEA2

The *PEA2* ORF was replaced precisely with *URA3* in vitro. First, a 2-kb ApaI–HindIII fragment of pNV22 was cloned into pBluescript SK (Strat-

agene, La Jolla, CA) digested with ApaI and HindIII to create plasmid pNV35. PCR amplification with two primers was used to generate a derivative of this plasmid which replaced the exact *PEA2* ORF with a SalI restriction site (pNV36). Each primer began with a 5′ SalI site and continued with *PEA2* flanking sequence, one of which began just 5′ to the ATG and was oriented towards the promoter, and the other of which began just 3′ to the stop codon and continued towards the 3′ untranslated region. PCR amplification with these primers yielded the entire plasmid sequence of pNV35 lacking the ORF; this fragment was digested with SalI and ligated to create pNV36. Finally, a 1.1-kb HindIII fragment of *URA3* (from YIp31) was introduced into the SalI site of pNV36 to create the *PEA2* disrupting plasmid pNV44 (Fig. 1 *D*).

Preparation of Pea2p-specific Antibodies

A peptide corresponding to the final carboxy 20 amino acids of Pea2p, preceded by a cysteine, was synthesized by the Biomolecular Resource Center (UCSF, San Francisco, CA) and had the following sequence: CK-NAEANTSLALNRDDPPDML. This peptide was coupled to keyhole limpet hemocyanin and antibodies were raised in two rabbits according to standard procedures (Caltag Laboratory, Healdsburg, CA).

The Pea2p peptide described above was coupled to BSA using glutaraldehyde for construction of a Pea2 peptide affinity column (Harlow and Lane, 1988). Whole serum was first adsorbed against a cyanogen bromide–activated Sepharose column coupled to whole cell extract of the *pea2Δ* strain (NVY201). Flowthrough from this column was then applied to a column of Affi-Gel 10/15 coupled to the peptide-BSA conjugate. Antibodies were eluted with 0.2 M glycine, pH 2.5, and collected in 2 M Tris, pH 9. The affinity-purified antibody was stored at −80°C.

Cell Extracts and Western Blots

Cells were grown to early log phase, centrifuged, washed with water, and resuspended in lysis buffer of 50 mM Tris, pH 7.5, 1% SDS, 5 mM DTT, 1 mM EDTA, and 1 mM PMSF. Samples were heated to 95°C for 5 min, mixed with glass beads, vortexed three times for 30 s each, and heated again to 95°C for 5 min. Protein concentrations were determined (Markwell et al., 1978) and equal amounts (typically 100 μg protein) loaded onto SDS polyacrylamide gels. Proteins were transferred to nitrocellulose, blocked for 2 h in 6% nonfat dry milk in TBST, and incubated overnight with a 1:2,000 dilution of the anti-Pea2p affinity-purified antibody or a 1:20,000 dilution of the anti-Spa2p antiserum (M. Snyder, Yale University, New Haven, CT). Immunoreactivity was visualized using the ECL protein detection kit (Amersham Corp., Arlington Heights, IL). The immunoblot of Pea2p (Fig. 3 *A*) includes two background bands caused by the secondary antibody: these bands were seen in all protein extracts blotted with three different primary antibodies.

Immunofluorescence

Immunofluorescence techniques were essentially as described (Pringle et al., 1989). Cells were grown to early log phase and fixed with formaldehyde for 1 h. Spheroplasted cells were attached to polylysine-coated slides and further permeabilized by incubation with 0.2% SDS for five min. Cells were blocked in 1% BSA for 1 h, incubated with anti-Pea2p antibodies (1:80 dilution) or anti-Spa2p antibodies (1:400 dilution) for 2 h, and finally incubated with Cy3-conjugated secondary anti–rabbit antibodies (1:100) for 1 h. Cells were photographed on a Zeiss axioscope using TMAX 400 film.

Results

PEA2 Encodes a Novel Protein

PEA2 was cloned by complementation of the mating defect of the *pea2-1* mutant (as described in Materials and Methods). The minimal complementing fragment was flanked by two SauIIIA restriction sites (Fig. 1, *A* and *C*) and carried two possible ORFs, which partially overlapped in opposite orientations (Fig. 1 *B*). To determine whether the larger ORF was *PEA2*, a frameshift mutation which affected only the larger ORF was introduced (Fig. 1 *B*; see Materials and Methods). When this plasmid was integrated into a *pea2-1* or *pea2-2* mutant, it no longer complemented the shmoo morphology or mating defect (data not shown). These results confirm that the larger ORF is *PEA2*.

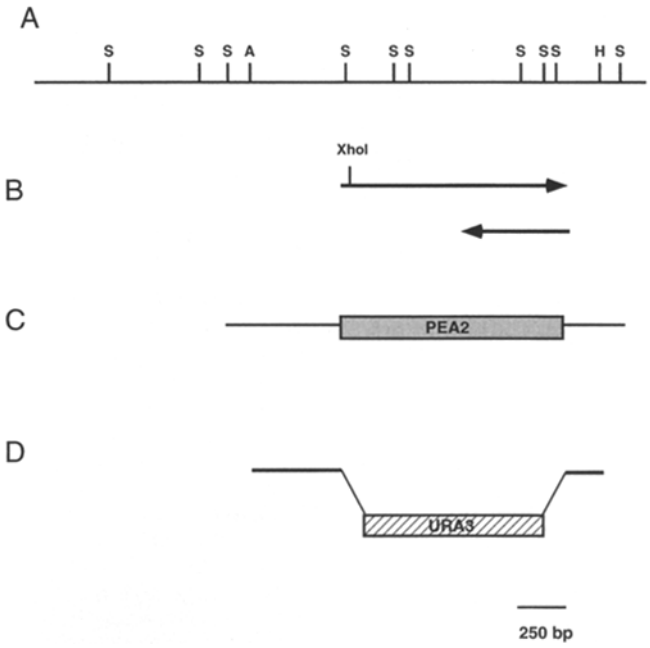

Figure 1. PEA2 encodes a novel protein. (*A*) Restriction map of the *PEA2* locus (S, SauIIIA; A, ApaI; H, HindIII). (*B*) Position of two ORFs contained on the complementing plasmid pNV22. A frameshift mutation was inserted at the XhoI site as indicated (pNV34) to ascertain which ORF contained the complementing activity. (*C*) *PEA2* ORF and flanking sequences carried on the minimal complementing plasmid pNV22. (*D*) *PEA2* deletion construct, which precisely replaces the *PEA2* ORF with a 1.1-kb fragment carrying *URA3*.

The *PEA2* gene encodes a protein of 420 amino acids, with a predicted molecular mass of 48.2 kD and a predicted coiled-coil domain. Part of the *PEA2* sequence is homologous to parts of many myosin molecules. A program which predicts the ability of a given sequence to form coiled coils (COILS version 2.1; Lupas et al., 1995) was used to analyze the *PEA2* sequence (Brown, J., personal communication). This sequence clearly indicates an ability to form a coiled coil between residue 236 and residue 327, with a stutter in the heptad repeat at residue 262; this analysis was confirmed by visual inspection of the sequence (Brown, J., personal communication). The 5′ upstream region does not appear to contain any pheromone response elements (PREs).

PEA2 Is Required for Shmoo Formation and Efficient Mating

To determine the null phenotype of *pea2* mutants, we constructed a complete deletion of the *PEA2* ORF (Fig. 1 *D*). **a**, α, and **a**/α *pea2Δ* mutants were viable and exhibited no growth or morphological defects under the conditions studied (YEPD and minimal SD media, 16°C, 30°C, and 37°C; Fig. 2). The *pea2Δ* strain was compared to the wild-type parent and to the original mutants, *pea2-1* and *pea2-2*, for its shmoo morphology and mating. After 2 h in the presence of pheromone, wild-type **a** cells formed pear-

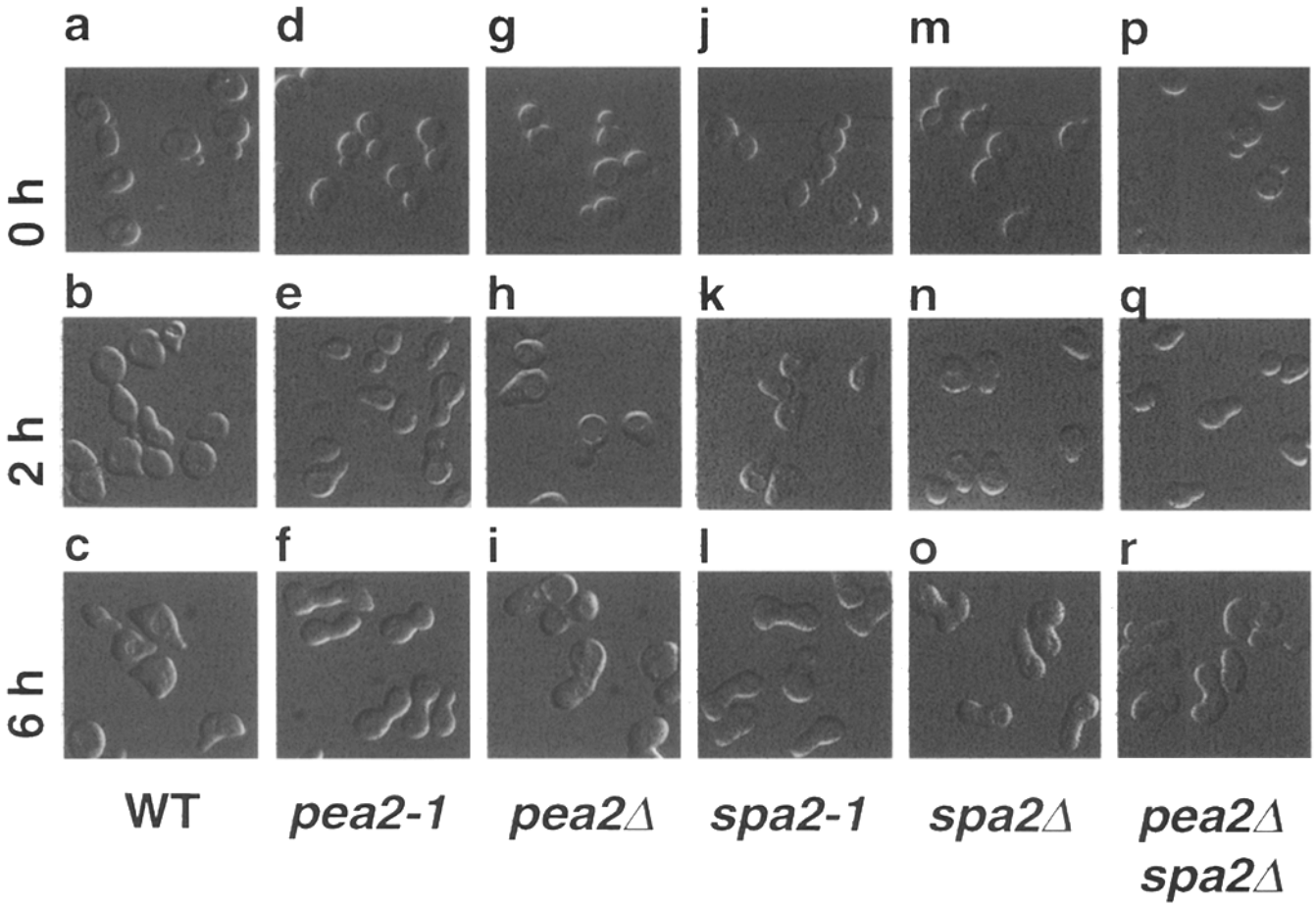

Figure 2. Shmoo morphologies of peanut mutants. **a** cells were treated with α factor for 0, 2, or 6 h. Cells of isogenic strains were as follows: (*a–c*) wild type (JC2-1B); (*d–f*) *pea2-1* (NVY6); (*g–i*) *pea2Δ* (NVY201); (*j–l*) *spa2-1* (NVY7); (*m–o*) *spa2Δ* (NVY139); (*p–r*) *pea2Δ spa2Δ* (NVY243).

shaped shmoos (Fig. 2 *b*). 4 h later, most wild-type cells extended a second or third shmoo tip, each relatively tight and small (Fig. 2 *c*). The shmoo tips seen in *pea2-1* and *pea2Δ* mutants were similar to wild-type after 2 h in pheromone although their shmoo tips already appeared slightly broader (Fig. 2, *e* and *h*). However, after 6 h in pheromone, the *pea2-1* and *pea2Δ* mutants exhibited dramatic peanut-shaped morphologies (Fig. 2, *f* and *i*). These shmoos appeared to have continued growth at the original shmoo tip instead of choosing a second site for polarization. In addition, the typical *pea2-1* and *pea2Δ* shmoos had much wider necks than normal shmoos; this difference can be seen to a lesser degree at the earlier time. There was no obvious difference in the kinetics of initial shmoo formation between the *pea2-1* and *pea2Δ* mutants and wild-type cells. Similar shmoo morphologies were exhibited by *pea2-2* mutants (data not shown).

The mating efficiencies of the *pea2* mutants were determined. Wild-type **a** cells mated to a wild-type α partner with an efficiency of 52% (Table II). **a** cells carrying *pea2-1, pea2-2*, and *pea2Δ* exhibited a somewhat reduced mating efficiency, 26–45% (Table II). A more pronounced mating defect was seen when *pea2* mutants were mated to an enfeebled mating partner carrying *far1-c* (Chenevert et al., 1994). Wild-type cells mate to *far1-c* strains with an efficiency of 6.5% (Table II). The *pea2* mutants exhibited mating efficiencies of 0.27–1.2% (Table II). Similar quantitative defects were seen when α *pea2* mutants were mated to **a** strains (data not shown). The mating defect of the *pea2Δ* mutant confirms that *PEA2* is required for efficient mating. Because the *pea2-2* mutant had a similar mating defect and shmoo morphology as a *pea2* deletion strain, we conclude that this allele is functionally null; *pea2-1* is a weaker allele, as it mates with slighty improved efficiency to an α *far1-c* mating partner (Table II).

SPA2 Is Required for Shmoo Formation and Efficient Mating

spa2Δ mutants have been previously described as unable to shmoo, instead forming mostly enlarged, ovoid, unpolarized cells in the presence of pheromone (Gehrung and Snyder, 1990). In contrast, the *spa2* mutants that we isolated (which carry mutations *spa2-1* and *spa2*-2) formed peanut-shaped shmoos (Fig. 2, *j–o*). This difference in phenotype might be due to the nature of the *spa2* mutations that we isolated or to differences in strain background or experimental conditions. To determine the phenotype of a *spa2Δ* mutant in our strain background, we constructed a complete deletion of *SPA2* using a knockout plasmid (p210,

Table II. Quantitative Mating of Peanut Mutants

*MAT*a strain	Relevant genotype	Mating to α wild type	Mating to α *far1-c*
		%	%
NVY193	WT	52	6.5
NVY226	*pea2-1*	45	1.2
NVY222	*pea2-2*	26	0.29
NVY200	*pea2Δ*	32	0.27
NVY230	*spa2-1*	34	0.82
NVY233	*spa2-2*	45	0.46
NVY207	*spa2Δ*	51	0.80
NVY244	*pea2Δ spa2Δ*	42	1.1

provided by M. Snyder). The morphology of this *spa2Δ* strain (Fig. 2, *n* and *o*) was indistinguishable from the *spa2-1* mutant (Fig. 2, *k* and *l*) and the *spa2-2* mutant (data not shown): all formed peanut-shaped shmoos. The *spa2Δ* mutant also mated at similar levels as the *spa2-1* and *spa2-2* mutants, whether mated to wild-type cells (34–51%) or to *far1*-c cells (0.46–0.82%; Table II).

To explore the difference between unpolarized and peanut-shaped shmoos, we further characterized the morphology of a *spa2Δ* mutant in the original Snyder background (MSY604), which was reported to yield a shmooless phenotype in the presence of pheromone (Gehrung and Snyder, 1990). We found that the morphology of this *spa2Δ* strain depended on two factors: the concentration of pheromone and the length of time of exposure to pheromone (data not shown). The *spa2Δ* mutant exhibited unpolarized, ovoid cells at shorter times and at lower concentrations of pheromone. However, as the cells were left longer in pheromone, and in the presence of higher pheromone concentrations, peanut-shaped shmoos were seen. Under every condition tested, the pheromone-induced morphologies of a *pea2Δ* mutant in the same background mirrored the *spa2* morphologies.

Because the *pea2Δ* and *spa2Δ* mutants have identical phenotypes, it was not possible to carry out an epistasis test. However, we did determine whether a cell lacking both Pea2p and Spa2p exhibited a more severe phenotype by constructing a strain with deletions in both genes. The *pea2Δ* spa2Δ double mutant exhibited a shmoo morphology (Fig. 2, *q* and *r*) and mating efficiencies (42.3% to wild-type, 1.1% to *far1-c*; Table II) similar to both single mutants.

PEA2 Is Required for the Bipolar Budding Pattern

a/α diploid cells that lack Spa2p are defective in bipolar budding (Snyder, 1989; Zahner et al., 1996). **a**/α diploid cells bud in the bipolar pattern, from either end of the cell. A newly born diploid daughter cell almost always positions its first bud distal to the site where it was attached to the mother cell (Chant and Pringle, 1995). Detailed analysis of **a**/α *spa2/spa2* mutants revealed a subtle variation of this pattern: newly born *spa2Δ* daughter cells correctly position the first bud at the distal pole but exhibit randomly placed buds in subsequent cell divisions. This phenotype is also exhibited by mutants defective in the *BUD6* gene (Zahner et al., 1996). Another mutation which specifically disrupts the bipolar budding pattern, *bni1*, causes defects in positioning of all diploid buds (Zahner et al., 1996). Mutants defective in *spa2*, *bud6*, and *bni1* all exhibit wild-type axial budding in haploid cells.

Because *pea2* and *spa2* mutants exhibit similar defects in mating, we were interested in determining if *pea2* mutants also exhibited defects in their budding pattern. Haploid *pea2* and *spa2* mutants exhibited the axial budding characteristic of haploid cells, as determined by Calcofluor staining of bud scars (Table III). These results show that *PEA2* does not play a role in axial bud site selection and confirm that *SPA2* is not required for axial budding, as shown previously (Zahner et al., 1996). In contrast, the bipolar budding pattern clearly depends upon both *PEA2* and *SPA2*. The budding pattern of homozygous diploid mutants was determined by counting cells with more than three bud scars, visualized by Calcofluor staining. Because *spa2* mutants choose the correct position for the first bud, it was important to only count cells with multiple bud scars. Wild-type diploid cells preferentially exhibited the bipolar budding pattern (85% bipolar; 15% nonbipolar). However, *pea2* mutants were dramatically reduced in their use of the bipolar budding pattern (65% nonbipolar) and had a defect comparable to *spa2* mutants (73% nonbipolar). An even stronger defect was seen for another bipolar-specific mutant, *bni1* (87% nonbipolar).

Having determined that *pea2* mutants have a bipolar budding pattern defect, we then determined whether these mutants (like *spa2* mutants) can correctly position the first bud (Table IV). Wild-type diploid daughter cells positioned the first bud at the pole distal to the birth scar 96% of the time, as expected. *spa2* diploids exhibited the wild-type pattern (89% distal) as did *pea2Δ* diploids (94% distal). A third bipolar budding pattern mutant, *bni1*, positioned the first daughter bud apparently randomly (36% distal, 50% equatorial, and 14% proximal). These results show that *pea2* and *spa2* mutants exhibit the same, specific budding pattern defect: mutants defective in either gene are defective in bipolar budding, although the first bud is correctly positioned. Neither gene is required for the axial budding pattern.

Table III. Budding Patterns of Peanut Mutants

Strain	Relevant genotype	Axial	Nonaxial
		%	%
NVY192	α WT	98	2
NVY193	**a** WT	99	1
NVY199	α *pea2Δ*	99	1
NVY200	**a** *pea2Δ*	98	2
NVY204	α *spa2Δ*	99	1
NVY207	**a** *spa2Δ*	99	1
NVY238	α *bni1Δ*	99	1
NVY239	**a** *bni1Δ*	96	4
		Bipolar	Nonbipolar
		%	
JPY142	**a**/α WT	85	15
NVY210	**a**/α *pea2Δ/pea2Δ*	35	65
NVY208	**a**/α *spa2Δ/spa2Δ*	27	73
NVY242	**a**/α *bni1Δ/bni1Δ*	13	87

Table IV.

strain	relevant genotype	% distal	% equatorial	% proximal
JPY142	a/α WT	96%	3%	1%
NVY208	a/α *spa2Δ*	89	10	1
NVY210	a/α *pea2Δ*	94	5	1
NVY242	a/α *bni1Δ*	36	50	14

Pea2p Antibody Specificity

To further characterize *PEA2* and its relationship to *SPA2*, we generated polyclonal antibodies against the carboxy terminal 20 amino acids of Pea2p. Affinity-purified antibodies were tested for specificity on blots of total yeast protein (Fig. 3 *A*). A band of ~50 kD seen in extracts from wild-type cells was missing in *pea2Δ* strains. This molecular mass corresponded to the predicted size of Pea2p (48 kD). A band of the same size was recognized by serum from a second rabbit immunized with the same peptide; again, this band was recognized in extracts from wild-type cells but not *pea2Δ* strains (data not shown). Two cross-reacting bands were seen in all cell extracts blotted with three different primary antibodies, which indicates they are due to binding of the secondary antibody. These data suggest that both antibodies specifically recognize Pea2p. Finally, the band recognized by these antisera was missing in extracts from *pea2-1* strains and was only faintly visible in extracts from *pea2-2* strains, indicating that these mutations destabilize Pea2p or lead to production of an unstable fragment.

Expression of Pea2p and Spa2p in Peanut Mutants

PEA2 and *SPA2* share several striking features: mutants defective in either gene generate similar mating and budding pattern defects. To explore their relationship further, we examined the behavior of Pea2p in *spa2* mutants and the behavior of Spa2p in *pea2* mutants. As a first step in this analysis, we determined the expression levels of each protein in several mutant strains. Surprisingly, the *spa2Δ* mutants did not contain Pea2p (Fig. 3 *A*). Similar results were seen for both *spa2* alleles (*spa2-1* and *spa2-2*; Fig. 3 *A*). These results indicate that Spa2p is required to produce wild-type levels of Pea2p.

Expression of Spa2p was determined using a polyclonal antiserum. A band of ~180 kD (and a collection of degradation products) detected in wild-type cells was missing in a *spa2Δ* strain (Fig. 3 *B*). *pea2Δ* strains produced full-length, wild-type levels of Spa2p (and the same spectrum of breakdown products, Fig. 3 *B*); the same result was seen with extracts from *pea2-1* and *pea2-2* mutants (data not shown). The Spa2p recovered in these extracts was largely degraded: several lower molecular weight bands seen in wild-type extracts were missing in the *spa2Δ* mutant (Fig. 3 *B*). Most importantly, the pattern of degradation products was the same in wild-type and *pea2Δ* strains. Thus, unlike the production of Pea2p in *spa2* mutants, Spa2p is produced at wild-type levels in the absence of Pea2p.

Immunolocalization of Pea2p in Budding Cells

The affinity-purified anti-Pea2p antiserum was used to localize Pea2p within budding **a** and α haploid and **a**/α diploid cells. The same general pattern of staining was revealed in all cell types (Figs. 4 and 5) and was the same using antibodies from two rabbits (data not shown). No immunofluorescent staining was seen in the *pea2Δ* strain (Fig. 4 *b*). Taken together, these data indicate that the pattern of staining shown here reflects the distribution of Pea2p.

In vegetative haploid and **a**/α diploid cells, Pea2p local-

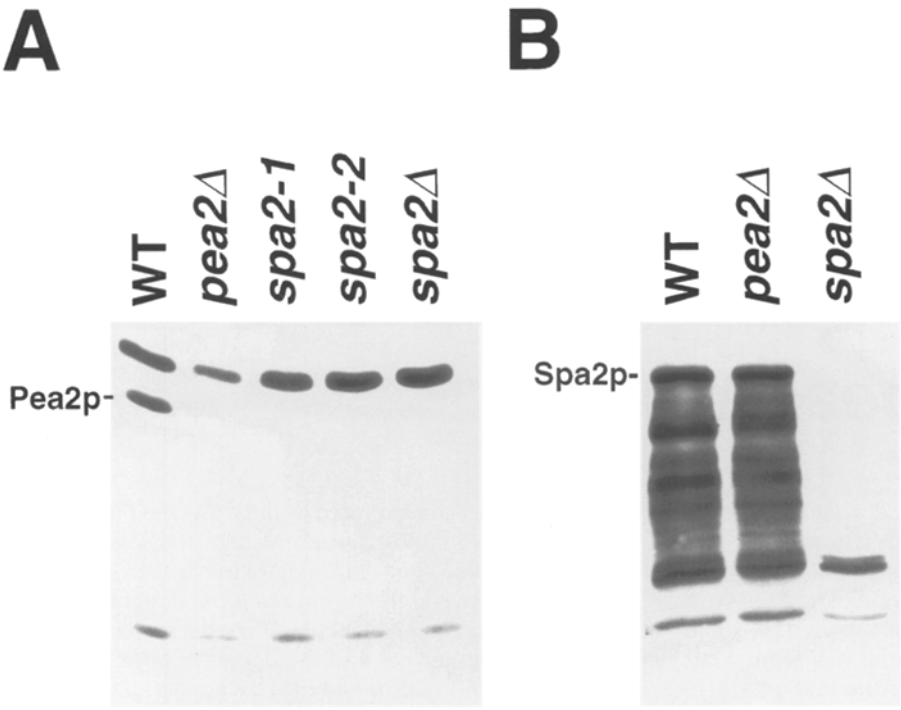

Figure 3. Production of Pea2p and Spa2p in *pea2* and *spa2* mutants. (*A*) Presence of Pea2p was determined by immunoblotting protein extracts prepared from isogenic strains NVY193 (**a** wild type), NVY200 (**a** *pea2Δ*), NVY7 (**a** *spa2-1*), NVY8 (**a** *spa2-2*), and NVY207 (**a** *spa2Δ*). Two background bands due to cross-reactivity of the secondary antibody are seen in all cell extracts (see Materials and Methods). (*B*) Spa2p expression was analyzed by immunoblotting protein extracts prepared from isogenic strains NVY193 (**a** wild type), NVY200 (**a** *pea2Δ*), and NVY207 (**a** *spa2Δ*).

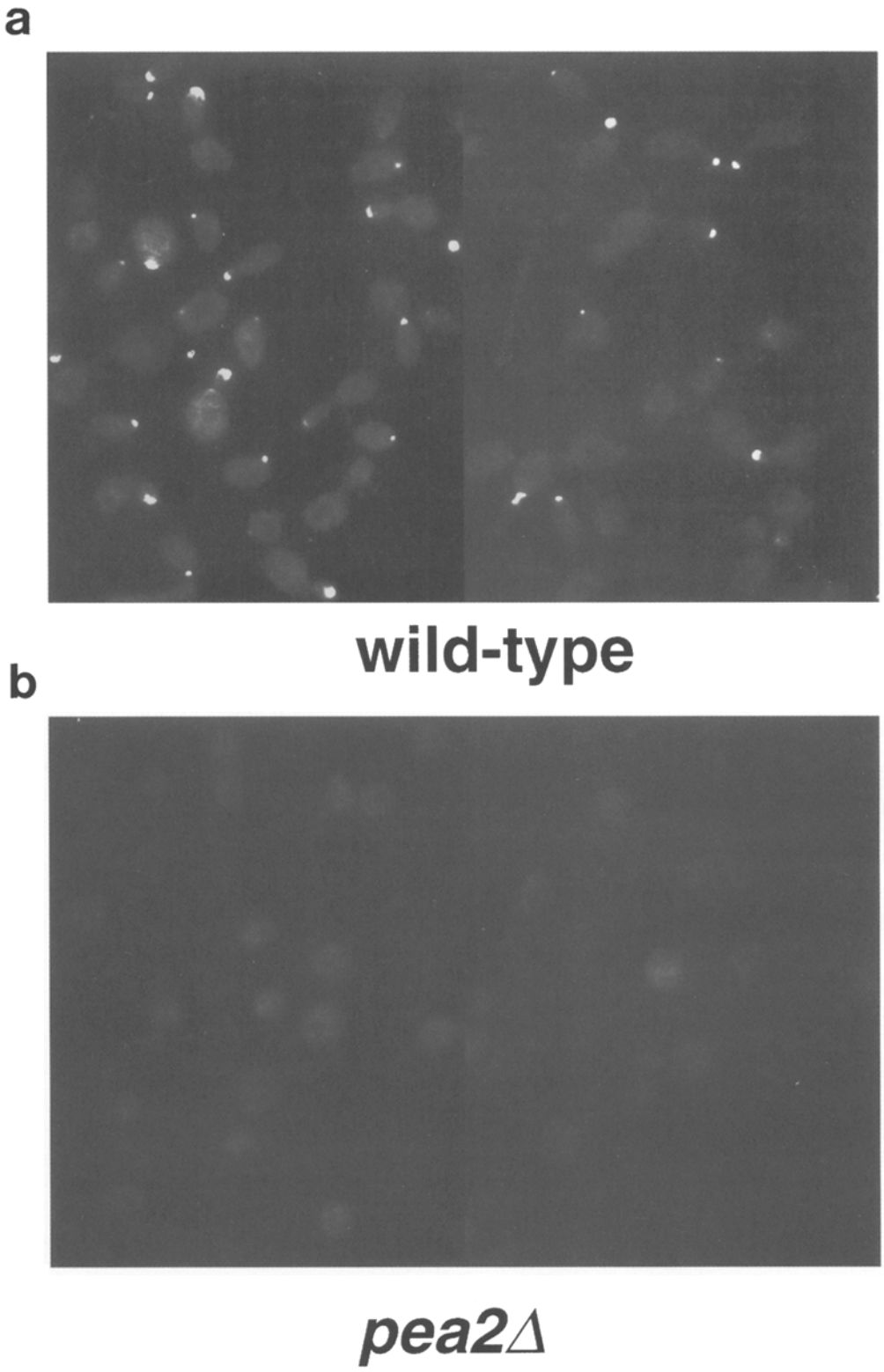

Figure 4. Localization of Pea2p in budding haploid cells. Cells of isogenic strains JC2-1B (**a** wild type) and NVY201 (**a** *pea2Δ*) were grown to early log phase and fixed. Localization of Pea2p was determined using indirect immunofluorescence with affinity-purified anti-Pea2p antibodies.

ized to sites of polarized growth (Figs. 4 *a* and 5). In unbudded cells, Pea2p staining appeared as a single patch (Figs. 4 *a* and 5 *a*). We interpret this stained area as the presumptive bud site because this region colocalized with a clustered ring of actin patches (data not shown). In small budded cells, the patch of Pea2p staining was seen to almost fill the bud (Figs. 4 *a* and 5 *b*). As the bud enlarged, Pea2p remained concentrated at the tip of the bud (Figs. 4 *a* and 5 *c*). Later in mitosis after nuclear division (as judged by DAPI staining) but before cytokinesis, Pea2p localized to the neck between the mother and the daughter cell, apparently as two rings or patches (Figs. 4 *a* and 5 *d*). During cytokinesis, the mother and the daughter both inherited a patch of Pea2p (Fig. 5, *d* and *e*). This general pattern of lo-

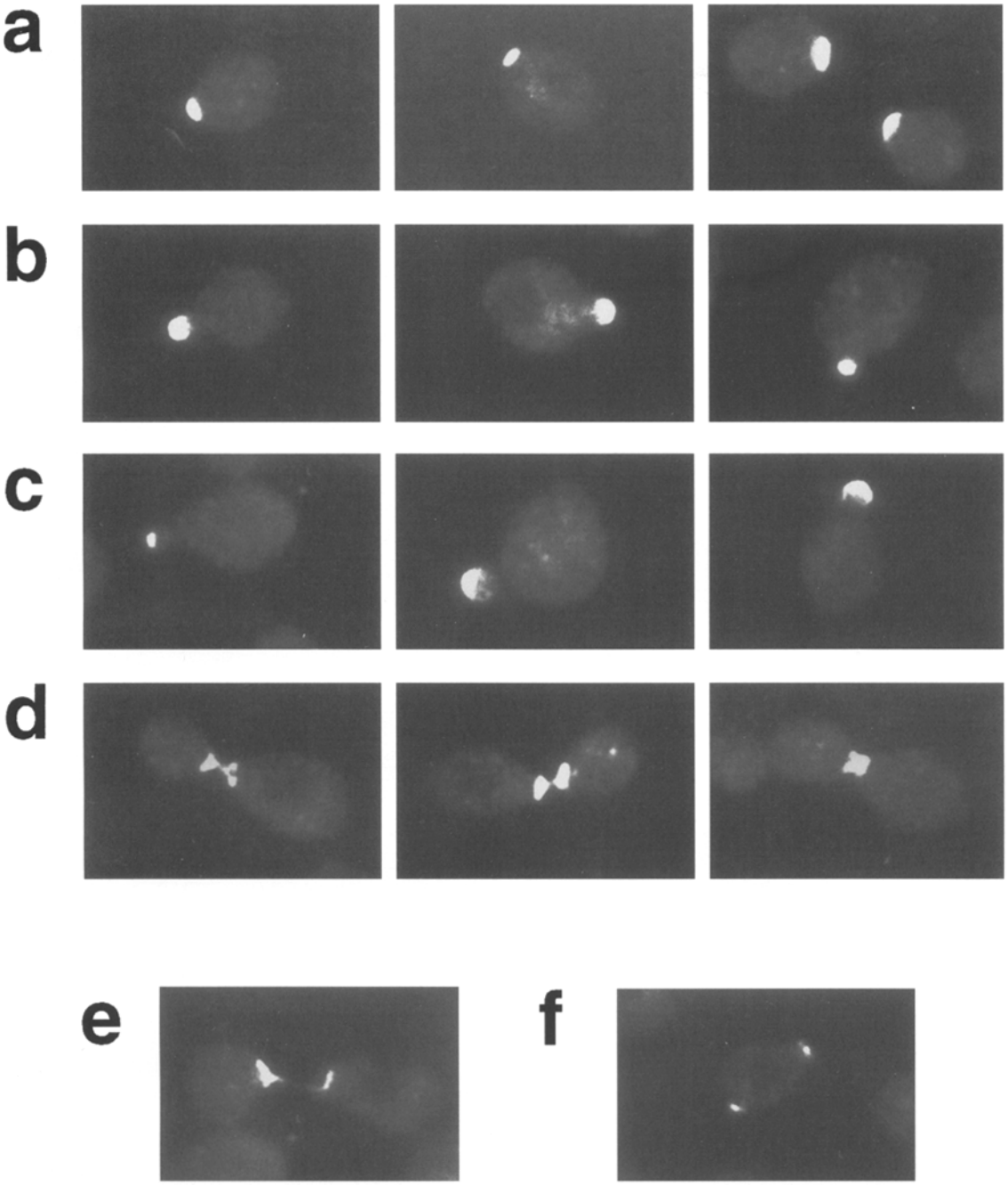

Figure 5. Localization of Pea2p in budding **a**/α diploid cells. Wild-type **a**/α diploid cells (JPY142) were grown to early log phase and processed for indirect immunofluorescence with affinity-purified anti-Pea2p antibodies. Shown here are examples of Pea2p staining in unbudded cells (*a*), small budded cells (*b*), medium budded cells (*c*), mitotic cells (*d*), two cells undergoing cytokinesis (*e*), and an unbudded cell with two patches of Pea2p (*f*).

calization is identical to that of Spa2p (Snyder, 1989; Snyder et al., 1991).

The only detectable difference in Pea2p localization between budding haploid and **a**/α diploid cells is shown in Fig. 5 *f*. Unbudded diploid cells were occasionally seen with two patches of Pea2p staining, one at either pole. Our interpretation of this pattern is that one patch was inherited from the mother at the neck region (see Fig. 5 *e*) and the other reflects the presumptive bud site (Fig. 5 *a*). This pattern was not seen in unbudded haploid cells, which form a bud adjacent to the previous site of division. If Pea2p were to localize to both old and new budding sites at the same time, it seems unlikely that we would be able to resolve two patches of staining because the previous and future bud sites are so close. Cells with two patches of staining have been seen for other proteins which localize to sites of polarized growth, including Spa2p (Snyder et al., 1991) and Myo2p (Lillie and Brown, 1994). Similarly, two rings of actin patches can occasionally be found in diploid cells at either end of the cell, again reflecting the previous

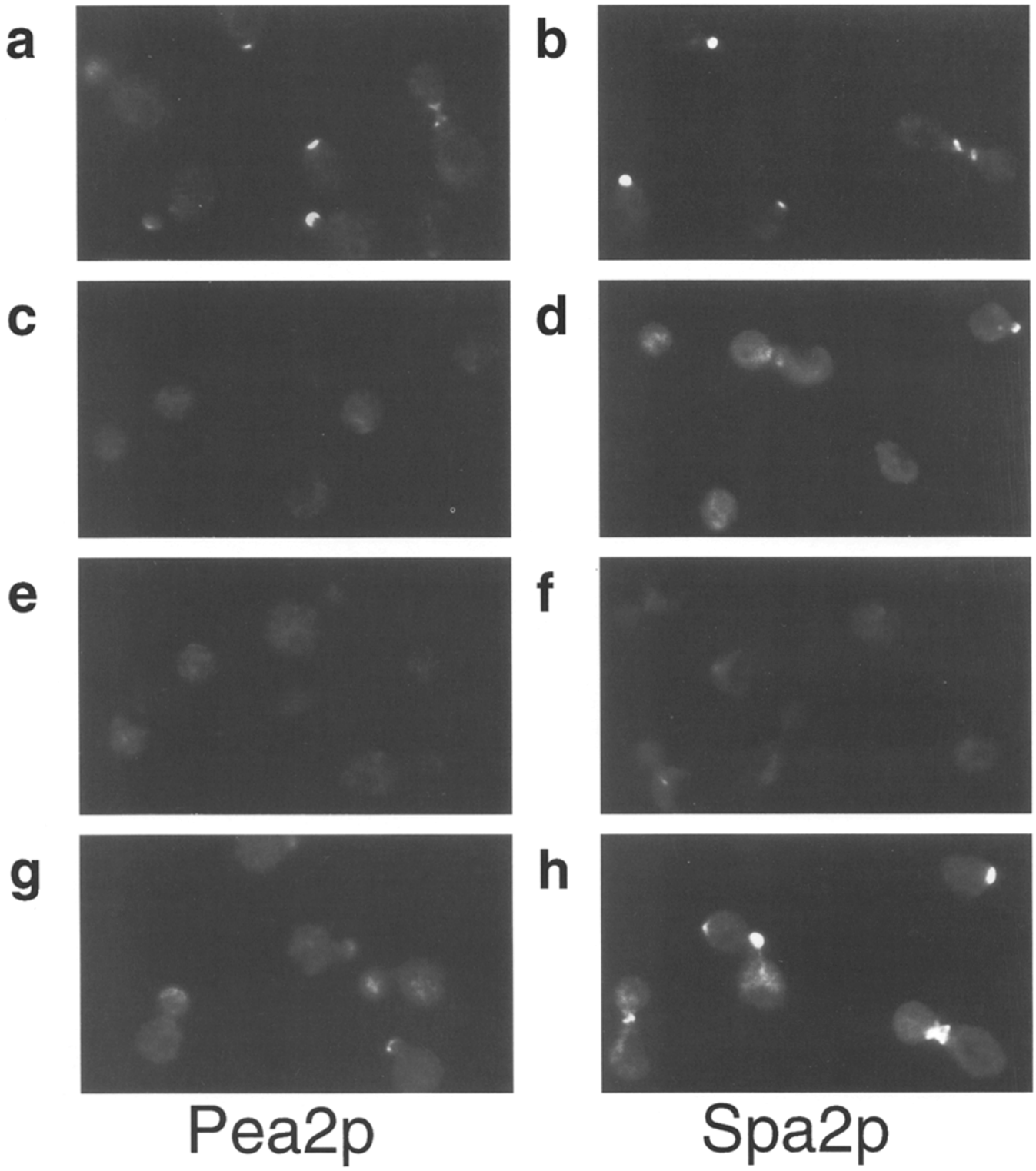

Figure 6. Localization of Pea2p and Spa2p in **a**/α diploid mutants defective in the bipolar budding pattern. Cells were grown to early log phase and processed for indirect immunofluorescence using anti-Pea2p antibodies (*left column*) or anti-Spa2p antibodies (*right column*) for the following isogenic strains: (*a–b*) JPY142 (**a**/α wild type); (*c–d*) NVY210 (**a**/α *pea2Δ/pea2Δ*); (*e–f*) NVY208 (**a**/α *spa2Δ/spa2Δ*); and (*g–h*) NVY242 (**a**/α *bni1Δ/bni1Δ*).

site of cell division and the presumptive bud site (Lillie and Brown, 1994).

Immunolocalization of Pea2p and Spa2p in Mutants Defective in PEA2, SPA2, or BNI1

PEA2, *SPA2*, and *BNI1* are required for the bipolar budding pattern exhibited by **a**/α diploid cells. We next asked whether mutations in these genes affected the localization of Pea2p and Spa2p in diploid cells. Wild-type **a**/α cells localized Pea2p and Spa2p to sites of polarized growth (Fig. 6, *a* and *b*). As expected, the *pea2Δ* mutant showed no Pea2p staining (Fig. 6 *c*), and a *spa2Δ* mutant showed no Spa2p staining (Fig. 6 *f*). Surprisingly, very little Spa2p localized in the *pea2Δ* mutant (Fig. 6 *d*); this result is especially striking as this mutant produces wild-type levels of Spa2p (Fig. 3 *b*). No Pea2p staining was seen in the *spa2Δ* mutant (Fig. 6 *e*); however, this mutant does not produce stable Pea2p (Fig. 3 *a*). Both Pea2p and Spa2p were properly localized in the bipolar budding mutant *bni1Δ* (Fig. 6, *g* and *h*), although fewer cells were stained with either antibody, and the intensity of the Pea2p staining was modestly reduced. These results demonstrate that proper localization of Pea2p and Spa2p depends on the presence of both wild-type proteins. Their nonlocalization cannot be ascribed to a defective bipolar budding pattern, because the bipolar budding mutant *bni1Δ* correctly localizes both proteins.

Immunolocalization of Pea2p and Spa2p in Shmoos

We were interested in determining the localization of Pea2p and Spa2p in shmoos because both *PEA2* and *SPA2* are required for proper shmoo morphogenesis and efficient mating. We first determined the localization of Pea2p in shmoos. A single patch of Pea2p staining was seen at the tip of the growing shmoo (Fig. 7 *a*). No Pea2p staining was seen in a *pea2Δ* strain (Fig. 7 *c*). The localization of Spa2p in a wild-type strain was identical to that previously reported (Snyder, 1989): Spa2p, like Pea2p, was found at the tip of the shmoo (Fig. 7 *b*). Spa2p was not localized in cells deleted for *pea2* (Fig. 7 *d*), although the *pea2Δ* mutant expressed wild-type levels of Spa2p (Fig. 3 *b*). This result is consistent with the nonlocalization of Spa2p in **a**/α *pea2Δ*/*pea2Δ* mutants (Fig. 6 *d*). Occasionally, a small amount of Spa2p was found at the shmoo tip; positively staining cells, however, were rare (<4%) and showed greatly reduced intensity, suggesting that the majority of Spa2p did not localize in *pea2* mutants. Similar observations were made for *pea2-1* and *pea2-2* mutants (data not shown). Because Pea2p is not present in *spa2* mutant shmoos (data not shown), we did not expect to find any Pea2p immunofluorescence in these cells, and indeed no staining was detected (Fig. 7 *e*). These results strongly suggest that the localization of Pea2p and Spa2p in shmoos is interdependent, and mirror the results for the localization of these two proteins in vegetative **a**/α *pea2/pea2* and *spa2/spa2* mutants (Fig. 6).

Discussion

Budding yeast relies on polarized growth during two phases of its life cycle, vegetative growth and mating. We have shown here that Pea2p is a novel protein that appears to function in close conjunction with Spa2p to contribute to cellular polarization during both budding and mating. During mating, Pea2p and Spa2p are required for proper polarization and efficient mating. During budding, Pea2p and Spa2p are required for the bipolar budding pattern of **a**/α diploid cells and appear to define a distinctive class of proteins involved in bud-site selection that includes Bud6p. Mutations in any of these genes lead to a novel mutant budding pattern: **a**/α diploid cells place the first bud in the correct, distal position but place subsequent buds at random positions. Pea2p and Spa2p are localized to sites of polarized growth in budding and shmooing cells. Each protein relies upon the presence of the other for its localization. These results suggest that Pea2p and Spa2p function together as a complex to generate cell polarity during two phases of the yeast life cycle.

The Role of Pea2p and Spa2p in Generating Polarized Morphogenesis during Mating

Mutants defective in *PEA2* and *SPA2* show identical defects in shmoo formation. Wild-type **a** cells exposed to pheromone initially form pear-shaped shmoos with a pointed tip. After several hours, they abandon growth at the original shmoo tip and initiate a second tip at another site on the cell surface. *pea2* and *spa2* mutants initially form a pear-shaped shmoo, although the tip is less pointed than that of wild-type cells. After several more hours in the presence of pheromone, the defect of these mutants becomes increasingly pronounced, leading to a broadened and enlarged shmoo which is shaped like a peanut. Mutants defective in both *pea2* and *spa2* can initiate a second shmoo tip after prolonged incubation (Valtz, N., unpublished data).

To understand the possible roles of *PEA2* and *SPA2*, we first considered how wild-type cells are thought to organize actin at a specific site. During mating, each haploid cell polarizes towards its mating partner: the actin cytoskeleton, secretion, and insertion of new cell wall material are all organized towards a single site on the cell surface (Byers, 1981; Ford and Pringle, 1986; Hasek et al., 1987; Tkacz and MacKay, 1979). Polarized morphogenesis is also seen in **a** cells in a uniform field of pheromone (Lipke et al., 1976; Tkacz and MacKay, 1979; Field and Schekman, 1980), but instead of polarizing towards a mating partner, the cell polarizes adjacent to the previous bud site (Madden and Snyder, 1992; Valtz et al., 1995). Generating polarity during mating and budding is thought to involve a hierarchy of three classes of gene products (Chant and Herskowitz, 1991; Chenevert, 1994). The site selection proteins mark the site for polarity on the cell surface and in turn organize the polarity establishment proteins (such as Bem1p, Cdc42p, and Cdc24p) towards that site. The polarity establishment proteins then organize actin and its associated proteins. The polarity establishment proteins and actin are involved in both budding and mating, whereas the site selection proteins are unique to each process (Chenevert, 1994). The end result of this morphogenetic pathway is polarization of actin at the chosen site, either the incipient bud site or the position of the mating partner.

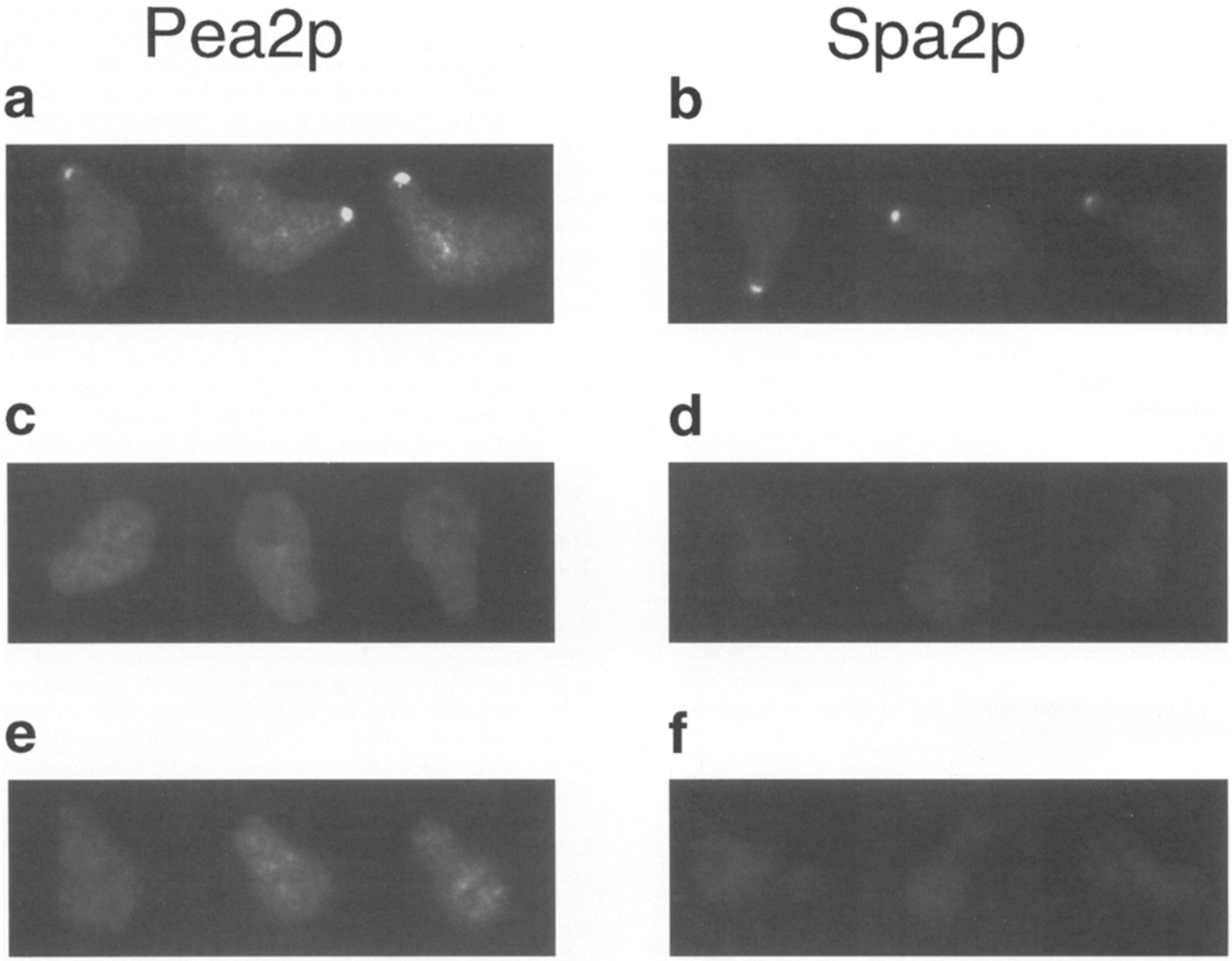

Figure 7. Localization of Pea2p and Spa2p in shmoos. Cells were grown to early log phase, treated with pheromone for 2.5 h, and processed for indirect immunofluorescence using anti-Pea2p antibodies (*left column*) or anti-Spa2p antibodies (*right column*). Isogenic strains were as follows: (*a–b*) **a** wild type (JC2-1B); (*c–d*) **a** *pea2Δ* (NVY201); and (*e–f*) **a** *spa2Δ* (NVY139).

There are several possible models for the role of *PEA2* and *SPA2* in polarized morphogenesis during mating. First, they may function to restrict the area initially selected for polarization. Thus, although they may function in conjunction with the site selection proteins, they would not themselves be required for correct site selection. This is consistent with the finding that mutants defective in *SPA2* are not defective in locating the mating partner (Dorer et al., 1995). Second, Pea2p and Spa2p may function in the organization of actin towards the chosen site; mutants lacking either protein may be unable to restrict actin structures to the site marked for polarization. A third possibility is that these proteins may function to maintain a tightly organized polarization site as new proteins and cell wall material are inserted; this model predicts that Pea2p and Spa2p play no role in choosing a correct site or establishing polarized actin in that direction. Finally, the enlarged shmoo tip seen in *pea2* and *spa2* mutants may reflect the mislocalization of a third protein whose localization depends on the presence of Pea2p and Spa2p; this unidentified protein could perform any of the functions described above.

The peanut-shaped shmoo morphology of *spa2Δ* mutants reported here differs from the ovoid shmooless phenotype previously described (Gehrung and Snyder, 1990). To determine the basis for this difference in phenotype, we have examined the *spa2Δ* strains described by Snyder which exhibit the unpolarized shmooless phenotype (Gehrung and Snyder, 1990). We observed that the degree of polarization exhibited by these mutants depended on the concentration of pheromone used as well as on how long the cells were exposed to pheromone. During shorter exposures and at lower concentrations, cells exhibited the ovoid morphology previously reported. However, extending the time in pheromone or increasing its concentration resulted in peanut-shaped shmoos. Polarized actin was observed in the ovoid cells (Gehrung and Snyder, 1990) as well as in the peanut-shaped shmoos (Valtz, N., unpublished data). Taken together, these results indicate that *SPA2* is not required to polarize actin in the presence of

pheromone but is important for the distribution of the actin cytoskeleton at the cell surface.

Precisely Organized Morphogenesis Appears to be Essential for Efficient Mating

Is the morphogenesis defect of *pea2* and *spa2* mutants responsible for their mating defect? Two observations suggest that these mutants mate poorly due to their defect in polarized growth. First, these mutants appear normal for other major events that occur during mating, including signal transduction, cell cycle arrest, and gene induction (Chenevert et al., 1994). Second, similar morphological defects are seen in mating mixes of *pea2* and *spa2* mutants, indicating that these defects are not simply an artifact of exposing cells to pheromone in the absence of a mating partner.

How might a defect in polarized morphogenesis lead to a mating defect? Polarized growth may function to guarantee localized deposition of mating-specific proteins involved in cell fusion, although the precise role of this polarization remains undefined. It is clear that correctly oriented polarization is required for efficient mating, as mutants which cannot locate the partner mate inefficiently (Jackson and Hartwell, 1990*b*; Dorer et al., 1995; Valtz et al., 1995). It may be important not only to choose the correct direction, but in addition, to have a precisely organized, small area of polarization in order to spatially define a restricted area for fusion. According to this view, the *pea2* and *spa2* mutants are defective in mating because fusogenic proteins are distributed over too broad a region and therefore lack a single area with a high enough concentration of the relevant proteins. Such an explanation is supported by the observation that mating of a *spa2* mutant to another *spa2* mutant is blocked before cell fusion and accumulates prefusion zygotes (Gammie, A., and M. Rose, M., personal communication). Similarly, a mating reaction of a *pea2* mutant to a wild-type partner accumulates 25-fold more prefusion zygotes than a wild-type mating reaction (Dorer, R., and L. Hartwell personal communication).

PEA2, SPA2, and BUD6 May Cooperate during the Establishment of the Bipolar Budding Pattern

The budding pattern of *pea2* and *spa2* mutants is curious. Wild-type **a**/α diploid cells bud in the bipolar pattern, in which newly born daughters always bud at the pole distal to the division site (the site of attachment to the mother; Chant and Pringle, 1995). Subsequent buds are positioned at either pole. Among the many genes required for this pattern, *PEA2*, *SPA2*, and *BUD6* form a distinct subset characterized by the mutant bipolar budding pattern displayed by mutants defective in these genes. This mutant pattern is typified by **a**/α *pea2/pea2* mutants, which correctly position the daughter's first bud in the wild-type position, distal to the division site, but then bud randomly.

To understand possible roles of *PEA2*, *SPA2*, and *BUD6*, we first consider what is known about establishment of the bipolar budding pattern. Although a direct search for genes required for bipolar budding was not carried out until recently (see below; Zahner et al., 1996), roles for many genes in bipolar budding have been discovered fortuitously, including *RVS161*, *RVS167* (Bauer et al., 1993; Sivadon et al., 1995), *SUR4*, *FEN1* (Durrens et al., 1993), *SPA2* (Snyder, 1989), and actin (Drubin et al., 1993; Yang, S., and D. Drubin, personal communication). A recent screen for mutations which disrupt the bipolar budding pattern identified several known genes (including *SPA2* and *BNI1*) and four new genes (*BUD6-9*; Zahner et al., 1996). Mutations in these genes disrupt the bipolar budding pattern in five distinguishable ways. (*1*) **a**/α *bud8/bud8* mutants bud only from the division site pole. (*2*) **a**/α *bud9/bud9* mutants bud only from the distal pole, opposite the birth scar. (*3*) **a**/α *bud7Δ*/bud7Δ mutants bud randomly but form short chains of bud scars reminiscent of the axial pattern. (*4*) **a**/α *bni1/bni1* mutants bud randomly. (*5*) **a**/α *pea2Δ/pea2Δ*, *spa2Δ/spa2Δ*, and *bud6/bud6* mutants all position the first daughter bud correctly at the distal pole and then bud at random.

These mutant phenotypes can be explained according to a model in which there are two landmarks for bipolar budding, one at the distal pole and one at the division site (Fig. 8; this model is a variant of model B in Chant and Pringle, 1995). Bud8p is a good candidate for the distal pole landmark and Bud9p is a good candidate for the division site landmark (Zahner et al., 1996). Bni1p and Bud7p may mediate recognition of the pole landmarks by Bud1p/Bud2p/Bud5p, which are required for both the bipolar and the axial patterns (Chant and Herskowitz, 1991; Chant et al., 1991).

Our challenge is to explain why Pea2p, Spa2p, and Bud6p are not required for positioning a daughter's first bud but are required thereafter (see also Zahner et al., 1996). We next consider in detail how the two pole landmarks might be deposited and possible roles for Pea2p, Spa2p, and Bud6p in this process. The landmark found at the distal tip of the daughter cell could be initially deposited at the presumptive bud site (Fig. 8 *a*) and remain at the bud tip as the cell grows (Fig. 8 *b*). A second landmark could be deposited at the mother/bud neck at mitosis (Fig. 8 *c*) and be partitioned to both the mother cell and the daughter cell (D1) during cytokinesis, marking the site of division (Fig. 8 *d*). The first bud produced by this daughter cell (D1) emerges at its distal tip (Fig. 8, *e* and *f*). When this cell divides, some division site landmark would be deposited at its distal pole (Fig. 8 *g*). Thus, after one division, both poles of the cell (D1) would be marked with the division site landmark (Fig. 8 *h*); this morphogenetic signal would be reinforced at the active pole each time it divides. No more distal pole landmark is deposited in a cell (D1) after its initial emergence, and the initially deposited distal pole landmark may itself decay over subsequent cell cycles. Thus, the distal pole landmark is essential for initially marking the distal pole, but its marking function is replaced by the division site landmark, which marks *both* poles after the initial bud emerges.

In this model, Pea2p, Spa2p, and Bud6p might function in the deposition of the division site landmark (Zahner et al., 1996). In the absence of these proteins, the distal pole landmark is correctly deposited as a daughter cell emerges (Fig. 8, *i–l*). However, as the newborn daughter cell goes on to divide, no division site landmark is deposited. In the absence of the division site landmark, a random budding pattern is observed in subsequent cell cycles after the initial distal pole landmark decays (Fig. 8, *m–p*). If the distal pole landmark decays over time, a preference for distal budding in the first few cell cycles would be expected; this

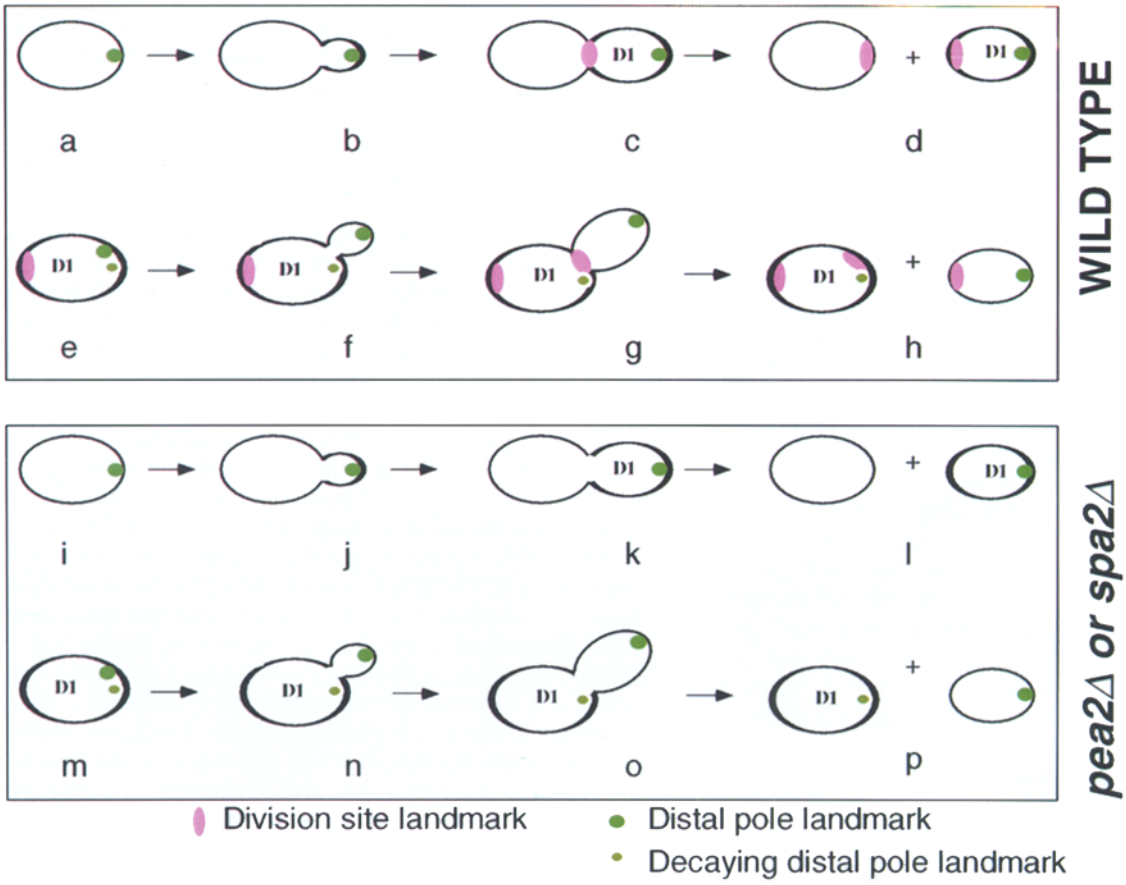

Figure 8. Model for establishment of the bipolar budding pattern: two different landmarks mark the two poles. A newly born daughter cell (D1) inherits bipolar budding landmarks at two positions during bud emergence. One landmark (indicated as the larger green dot; perhaps Bud8p) is deposited at the presumptive bud site (*a*) and carried to the tip of the growing bud (*b*) where it remains, resulting in a landmark distal to the division site (*d*). A second landmark (indicated in pink; perhaps Bud9p) is deposited at the mother/daughter neck during cytokinesis (*c*), resulting in a landmark at the division site (*d*). When the daughter cell (D1) buds for the first time, the bud emerges distal to the division site (*e* and *f*). At mitosis (*g*), the original daughter cell (D1) acquires some division site landmark at its new division site. The D1 cell now has division site landmark at both poles (*h*). Additional buds will lead to the continued deposition of the division site landmark in the D1 cell. In a *pea2* or *spa2* mutant, it is hypothesized that a division site landmark is not deposited (*i–p*). The distal pole landmark is deposited in D1 when it first emerges (*i* and *j*), but no division site landmark is deposited at mitosis (*k*). Thus, the newly born daughter cell D1 has correctly positioned distal pole landmark (*l*) and therefore correctly positions its first bud at the distal pole (*m* and *n*). Again, no division site landmark is deposited at mitosis (*o*). If the distal pole landmark is itself unstable (indicated as the smaller green dot), after one cell cycle D1 would have only its distal pole marked (*p*). This landmark may be present for only a few more cell cycles, leading to a cell with neither pole marked and consequently random budding.

has been observed for *spa2* and *bud6* mutants (Zahner et al., 1996). Another possibility is that these proteins may perform a more general role in maintaining or stabilizing the landmarks at either pole. The landmarks which mark the poles of a bipolarly budding cell persist over several cell cycles (Chant and Pringle, 1995). These landmarks may be deposited as a daughter cell emerges but require further modification for stability. Pea2p, Spa2p, and Bud6p may function in stabilizing the two pole landmarks. In this model, mutants defective in one of these genes would position the first bud correctly simply because the landmarks have not yet been destabilized. Finally, it is possible that Pea2p, Spa2p, and Bud6p are themselves components of the division site landmark.

Is there any evidence to suggest that Spa2p, Pea2p, and Bud6p function in deposition of the proximal landmark? The strongest argument is that mutants defective in these genes share a highly specific budding pattern phenotype. In addition, Pea2p and Spa2p are located at the mother/bud neck during mitosis, when the theoretical division site landmark is deposited. It will be interesting to determine if Bud6p is also localized to the mother/bud neck during mitosis as well as to determine if *bud6* mutants exhibit the shmooing and mating defects of *pea2* and *spa2* mutants.

Pea2p and Spa2p May Function as a Complex

The phenotypes displayed by mutants defective in *PEA2* and *SPA2* suggest that they are functionally related genes. First, both are required for wild-type shmoo formation as well as for efficient mating. Mutants defective in one or both genes have identical shmoo and mating defects, which suggests that these genes may function in the same aspect of polarized morphogenesis during mating. Second, both genes were identified in an independent screen (Yorihuzi et al., 1994) for mutants defective in shmoo formation (*PEA2*

is identical to *PPF2*; Dorer, R., and L. Hartwell, personal communication). Third, both genes are required for default mating in the absence of a pheromone gradient (Dorer et al., 1995; Dorer, R., and L. Hartwell, personal communication). Fourth, both genes are similarly required to establish the bipolar budding pattern in **a**/α diploid cells after the first daughter bud is positioned (Snyder, 1989; Zahner et al., 1996; this study). Fifth, both *PEA2* and *SPA2* are required for filamentous growth during pseudohyphal development (Mosch, M., and G. Fink, personal communication). Thus, for all known roles of one gene, a corresponding role has been found for the other.

The behavior of Pea2p and Spa2p further suggests that they interact directly. First, both proteins localize to sites of polarized growth. Although direct colocalization of Pea2p and Spa2p has not yet been carried out, the localization of both proteins to sites of growth as determined by actin staining suggests that they do colocalize. Second, the presence of Spa2p is necessary for Pea2p production. Third, Spa2p does not properly localize in the absence of Pea2p. Finally, both Pea2p and Spa2p are predicted to contain coiled-coil domains, which are potential sites of interaction. These genetic and biochemical observations suggest that Pea2p and Spa2p may form a complex which performs different roles in polarization during many phases of the yeast life cycle.

We thank J. Pringle and J. Chenevert for discussion; M. Snyder for antibodies, yeast strains, plasmids, and discussions; J. Brown and G. Petsko for sequence analysis of *PEA2*; C. Boone for a plasmid; D. Drubin, C. Boone, J. Pringle, H. Mosch, M. Rose, and R. Dorer for communication of unpublished results; and members of the Herskowitz Lab, Mating Club, UCSF Friends of Microtubules, and R. Dorer for their interest, helpful advice, and comments on the manuscript.

N. Valtz was supported by a graduate fellowship from the National Science Foundation and in part by National Institutes of Health (NIH) Genetics Training Grant. This work was supported by NIH research grant GM48052. We also gratefully acknowledge support from the Markey Foundation and from the Herbert W. Boyer Fund.

Received for publication 12 July 1996 and in revised form 20 August 1996.

References

Adams, A.E.M., and J.R. Pringle. 1984. Relationship of actin and tubulin distribution to bud growth in wild-type and morphogenetic mutant *Saccharomyces cerevisiae. J. Cell Biol.* 98:934–945.

Bauer, F., M. Urdaci, M. Aigle, and M. Crouzet. 1993. Alteration of a yeast SH3 protein leads to conditional viability with defects in cytoskeletal and budding patterns. *Mol. Cell. Biol.* 13:5070–5084.

Byers, B. 1981. Cytology of the yeast life cycle. *In* The Molecular Biology of the Yeast *Saccharomyces cerevisiae:* Life Cycle and Inheritance. J.N. Strathern, E.W. Jones, and J.R. Roach, editors. Cold Spring Harbor Laboratory Press, Cold Spring Harbor, NY. pp. 59–96.

Chant, J., and I. Herskowitz. 1991. Genetic control of bud site selection in yeast by a set of gene products that constitute a morphogenetic pathway. *Cell.* 65: 1203–1212.

Chant, J., and J.R. Pringle. 1995. Patterns of bud-site selection in the yeast *Saccharomyces cerevisiae. J. Cell Biol.* 129:751–765.

Chant, J., K. Corrado, J.R. Pringle, and I. Herskowitz. 1991. Yeast *BUD5*, encoding a putative GDP-GTP exchange factor, is necessary for bud site selection and interacts with bud formation gene *BEM1. Cell.* 65:1213–1224.

Chenevert, J. 1994. Cell polarization directed by extracellular cues in yeast. *Mol. Biol. Cell.* 5:1169–1175.

Chenevert, J., N. Valtz, and I. Herskowitz. 1994. Identification of genes required for pheromone-induced cell polarization in *Saccharomyces cerevisiae. Genetics.* 136:1287–1297.

Cross, F., L.H. Hartwell, C. Jackson, and J.B. Konopka. 1988. Conjugation in *Saccharomyces cerevisiae. Annu. Rev. Cell Biol.* 4:429–457.

Dorer, R., P.M. Pryciak, and L.H. Hartwell. 1995. *Saccharomyces cerevisiae* cells execute a default pathway to select a mate in the absence of pheromone gradients. *J. Cell Biol.* 131:845–861.

Drubin, D.G. 1991. Development of cell polarity in budding yeast. *Cell.* 65: 1093–1096.

Drubin, D.G., H.D. Jones, and K.F. Wertman. 1993. Actin structure and function: roles in mitochondrial organization and morphogenesis in budding yeast and identification of the phalloidin-binding site. *Mol. Biol. Cell.* 4:1277–1294.

Durrens, P., E. Revardel, M. Bonneu, and M. Aigle. 1995. Evidence for a branched pathway in the polarized cell division of *Saccharomyces cerevisiae. Curr. Genet.* 27:213–216.

Field, C., and R. Schekman. 1980. Localized secretion of acid phosphatase reflects the pattern of cell surface growth in *Saccharomyces cerevisiae. J. Cell Biol.* 86:123–128.

Ford, S., and J.R. Pringle. 1986. Development of spatial organization during the formation of zygotes and shmoos in *Saccharomyces cerevisiae. Yeast.* 2:S114.

Freifelder, D. 1960. Bud position in *Saccharomyces cerevisiae. J. Bacteriol.* 80: 567–568.

Gehrung, S., and M. Snyder. 1990. The *SPA2* gene of *Saccharomyces cerevisiae* is important for pheromone-induced morphogenesis and efficient mating. *J. Cell Biol.* 111:1451–1464.

Harlow, E., and D. Lane. 1988. Antibodies: A Laboratory Manual. Cold Spring Harbor Press, Cold Spring Harbor, NY. 726 pp.

Hasek, J., I. Rupes, J. Svobodova, and E. Streiblova. 1987. Tubulin and actin topology during zygote formation of *Saccharomyces cerevisiae. J. Gen. Microbiol.* 133:3355–3363.

Hicks, J.B., J.N. Strathern, and I. Herskowitz. 1977. Interconversion of yeast mating types. III. Action of the homothallism (*HO*) gene in cells homozygous for the mating type locus. *Genetics.* 85:395–405.

Huisman, O., W. Raymond, K. Froelich, P. Errada, N. Kleckner, D. Botstein, and M.A. Hoyt. 1987. A Tn*10-lacZ-kanR-URA3* gene fusion transposon for insertion mutagenesis and fusion analysis of yeast and bacterial genes. *Genetics.* 116:191–199.

Jackson, C.L., and L.H. Hartwell. 1990*a*. Courtship in *S. cerevisiae:* both cell types choose mating partners by responding to the strongest pheromone signal. *Cell.* 63:1039–1051.

Jackson, C.L., and L.H. Hartwell. 1990*b*. Courtship in *Saccharomyces cerevisiae*: an early cell-cell interaction during mating. *Mol. Cell. Biol.* 10:2202–2213.

Johnston, G.C., J.A. Prendergast, and R.A. Singer. 1991. The *Saccharomyces cerevisiae MYO2* gene encodes an essential myosin for vectorial transport of vesicles. *J. Cell Biol.* 113:539–551.

Kilmartin, J.V., and A.E.M. Adams. 1984. Structural rearrangements of tubulin and actin during the cell cycle of the yeast *Saccharomyces. J. Cell Biol.* 98:922–933.

Lillie, S.H., and S.S. Brown. 1994. Immunofluorescence localization of the unconventional myosin, Myo2p, and the putative kinesin-related protein, Smy1p, to the same regions of polarized growth in *Saccharomyces cerevisiae. J. Cell Biol.* 125:825–842.

Lipke, P.N., A. Taylor, and C.E. Ballou. 1976. Morphogenic effects of α-factor on *Saccharomyces cerevisiae* cells. *J. Bacteriol.* 127:610–618.

Lupas, A., S. Muller, K. Goldie, A.M. Engel, and W. Baumeister. 1995. Model structure of the OMP α rod, a parallel four-stranded coiled coil from the hyperthermophilic eubacterium *Thermotoga maritima. J. Mol. Biol.* 248:180–189.

Madden, K., and M. Snyder. 1992. Specification of sites for polarized growth in *Saccharomyces cerevisiae* and the influence of external factors on site selection. *Mol. Biol. Cell.* 3:1025–1035.

Markwell, M.A.K., S.M. Haas, L.L. Bieber, and N.N. Tolbert. 1978. A modification of the Lowry procedure to simplify protein determination in membrane and lipoprotein samples. *Anal. Biochem.* 87:206–210.

Pringle, J.R., R.A. Preston, A.E.M. Adams, T. Stearns, D.G. Drubin, B.K. Haarer, and E.W. Jones. 1989. Fluorescence microscopy methods for yeast. *Methods Cell Biol.* 31:357–435.

Rose, M.D., P. Novick, J.H. Thomas, D. Botstein, and G.R. Fink. 1987. A *Saccharomyces cerevisiae* genomic plasmid bank based on a centromere-containing shuttle vector. *Gene (Amst.).* 60:237–243.

Rose, M.D., F. Winston, and P. Hieter. 1990. Methods in Yeast Genetics: A Laboratory Course. Cold Spring Harbor Press, Cold Spring Harbor, NY. 123 pp.

Segall, J.E. 1993. Polarization of yeast cells in spatial gradients of α-mating factor. *Proc. Natl. Acad. Sci. USA.* 90:8332–8336.

Sivadon, P., F. Bauer, M. Aigle, and M. Crouzet. 1995. Actin cytoskeleton and budding pattern are altered in the yeast *rvs161* mutant: the Rvs161 protein shares common domains with the brain protein amphiphysin. *Mol. Gen. Genet.* 246:485–495.

Sloat, B.F., A.E.M. Adams, and J.R. Pringle. 1981. Roles of the *CDC24* gene product in cellular morphogenesis during the *Saccharomyces cerevisiae* cell cycle. *J. Cell Biol.* 89:395–405.

Snyder, M. 1989. The *SPA2* protein of yeast localizes to sites of cell growth. *J. Cell Biol.* 108:1419–1429.

Snyder, M., S. Gehrung, and B.D. Page. 1991. Studies concerning the temporal and genetic control of cell polarity in *Saccharomyces cerevisiae. J. Cell Biol.* 114:515–532.

Tkacz, J.S., and V.L. MacKay. 1979. Sexual conjugation in yeast. *J. Cell Biol.* 80: 326–333.

Valtz, N., M. Peter, and I. Herskowitz. 1995. *FAR1* is required for oriented polarization of yeast cells in response to mating pheromones. *J. Cell Biol.* 131:863–873.

Welch. M.D., D.A. Holtzman, and D.G. Drubin. 1994. The yeast actin cytoskeleton. *Curr. Opin. Cell Biol.* 6:110–119.

Yorihuzi, T., and Y. Ohsumi. 1994. *Saccharomyces cerevisiae MATa* mutant cells defective in pointed projection formation in response to α-factor at high concentrations. *Yeast* 10:579–594.

Zahner, J.A., H.A. Harkins, and J.R. Pringle. 1996. Genetic analysis of the bipolar pattern of bud site selection in the yeast *Saccharomyces cerevisiae. Mol. Cell. Biol.* 16:1857–1870.